

# Reheating Phase Diagram for Single-field Slow-roll Inflationary Models

Rong-Gen Cai,<sup>\*</sup> Zong-Kuan Guo,<sup>†</sup> and Shao-Jiang Wang<sup>‡</sup>  
*State Key Laboratory of Theoretical Physics, Institute of Theoretical Physics,  
 Chinese Academy of Sciences, Beijing 100190, China.*  
 (Dated: April 14, 2024)

We investigate the influence on the inflationary predictions from the reheating processes characterized by the  $e$ -folding number  $N_{\text{reh}}$  and the effective equation-of-state parameter  $w_{\text{reh}}$  during reheating phase. For the first time, reheating processes can be constrained in the  $N_{\text{reh}}-w_{\text{reh}}$  plane from Planck 2015. We find that for Higgs inflation with a non-minimal coupling to gravity, the predictions are insensitive to the reheating phase for current CMB measurements. We also find that the spontaneously broken SUSY inflation and axion monodromy inflation with  $\phi^{2/3}$  potential, which with instantaneous reheating lie outside or at the edge of 95% confidence region in the  $n_s-r$  plane from Planck 2015 TT,TE,EE+lowP, can well fit the data with the help of reheating processes. Future CMB experiments would put strong constraints on reheating processes.

## I. INTRODUCTION

Models of single-field slow-roll inflation with a standard kinetic term provide a very good fit to the Planck data [1, 2]. In the inflationary scenario, the universe expands quasi-exponentially as the scalar field rolls slowly along a very flat potential. After inflation ends, the inflaton field oscillates around the minimum of the potential. During such a period of reheating, the energy in the inflaton is transferred to the plasma of standard model particles. Reheating is an integral part of inflationary models. Without reheating the universe after inflation would be empty and cold. However, the physics of reheating may be more complicated. As pointed out in [3], the equation-of-state parameter changes sharply during reheating phase due to the out-of-equilibrium nonlinear dynamics of fields.

Predictions of slow-roll inflationary models are usually derived given a reasonable range for the  $e$ -folding number  $N_{\text{inf}}$  during inflation. With more and more precise CMB measurements [1, 2], it becomes important to consider the impact on the inflationary predictions from reheating processes [4–9]. It is pointed out that the reheating processes provide additional constraints on inflationary models via the reheating temperature [10] and some specific inflationary models are investigated in [11–13]. Although the physics of reheating is highly uncertain and unconstrained due to its non-linear backreaction and non-perturbative nature, the reheating phase can in principle be characterized by two parameters only: the  $e$ -folding number  $N_{\text{reh}}$  and the effective Equation-of-State (EoS) parameter  $w_{\text{reh}}$ . In terms of these two parameters one can express the observable quantities such as the scalar spectral index  $n_s$  and its running  $\alpha_s$ , tensor spectral index  $n_t$  and its running  $\alpha_t$ , tensor-to-scalar ratio  $r$ ,  $e$ -folding number  $N_{\text{inf}}$  and reheating temperature

$T_{\text{reh}}$ . Thus reheating processes can be constrained in the  $N_{\text{reh}}-w_{\text{reh}}$  plane by Planck constraints on  $n_s$  and  $r$ .

Following the approach proposed in [10–12], in this paper we study several models of single-field slow-roll inflation including Higgs inflation, power-law potential, hilltop inflation, natural inflation, Spontaneously Broken (SB) SUSY inflation and superconformal  $\alpha$ -Attractors. Although the reheating/preheating mechanisms are well studied in the Higgs inflation [14–16], the underlying mechanisms of unitarization and stabilization in Higgs inflation might have substantial impact on the reheating phase, as discussed in [17]. For Higgs inflation, we find that the inflationary predictions are insensitive to reheating processes given the current precision of CMB measurements. The same conclusion is also derived in Ref. [18]. We find that the SB SUSY inflation and power-law potential  $\phi^{2/3}$ , which lie outside or at the edge of 95% confidence region in the  $n_s-r$  plane from Planck 2015 TT,TE,EE+lowP, can well fit the data if reheating processes are taken into account. However the constrained parameter space of reheating processes is still very large for most of inflationary models due to current relatively weak constraints on inflation, future measurements of  $n_s$  and  $r$  will eventually narrow down the parameter space thus reveal the physics of reheating era.

The paper is organized as follows. In Section 2 we introduce the effective descriptions of reheating phase in terms of  $N_{\text{reh}}$  and  $w_{\text{reh}}$  for single-field slow-roll inflationary models. In Section 3 we study some specific inflationary models. Section 4 is devoted to conclusions.

## II. DESCRIPTIONS OF REHEATING PHASE

Firstly, following the method proposed in [10–12] we derive a formula for the effective number of degrees of freedom at the end of reheating phase. It is worth noting that one should not take this literally since most of observables are insensitive to the precise value of  $g_{\text{reh}}$  due to its logarithmic dependence. However the derived formula of  $g_{\text{reh}}$  will be essential to carry out the inflationary predictions in the  $N_{\text{reh}}-w_{\text{reh}}$  plane, which can be used

<sup>\*</sup> cairg@itp.ac.cn

<sup>†</sup> guozk@itp.ac.cn

<sup>‡</sup> schwang@itp.ac.cn

to constrain the parameter space of reheating phase to meet the current constraints on inflation.

The pivot scale is chosen as  $k_* = 0.002\text{Mpc}^{-1}$ , which is also expressed by

$$k_* = a_* H_* = \frac{a_*}{a_{\text{end}}} \frac{a_{\text{end}}}{a_{\text{reh}}} \frac{a_{\text{reh}}}{a_0} a_0 H_*. \quad (1)$$

In what follows, the current scale factor  $a_0 = 1$  and all quantities with subscript “\*” are evaluated at the moment when the pivot scale crosses the horizon.

The first two factors of (1) can be computed by

$$\frac{a_*}{a_{\text{end}}} \frac{a_{\text{end}}}{a_{\text{reh}}} = e^{-(N_* + N_{\text{reh}})}. \quad (2)$$

The third factor of (1) is computed as follows. We use the conservation equation of entropy  $g_{\text{reh}} a_{\text{reh}}^3 T_{\text{reh}}^3 = g_\gamma a_0^3 T_\gamma^3 + g_\nu a_0^3 T_\nu^3 = (43/11) T_\gamma^3 a_0^3$  by noting that  $g_\gamma = 2$ ,  $g_\nu = (7/8) \times 3 \times 2 = 21/4$ , and  $T_\nu^3 = (4/11) T_\gamma^3$ , here we adopt  $T_\gamma = 2.7255\text{K}$ . Thus the third factor can be written as

$$\frac{a_{\text{reh}}}{a_0} = \left( \frac{43}{11 g_{\text{reh}}} \right)^{\frac{1}{3}} \frac{T_\gamma}{T_{\text{reh}}}, \quad (3)$$

where the temperature  $T_{\text{reh}}$  at the end of reheating phase needs to be properly accounted for. Assuming that the whole history during reheating phase can be effectively described by the  $e$ -folding number  $N_{\text{reh}}$  and the effective EoS parameter  $w_{\text{reh}}$ , we are able to relate the reheating phase to the inflationary phase via

$$\rho_{\text{end}} = \frac{3}{3 - \epsilon_{\text{end}}} V_{\text{end}}, \quad (4)$$

$$\rho_{\text{reh}} = \rho_{\text{end}} e^{-3N_{\text{reh}}(1+w_{\text{reh}})}, \quad (5)$$

$$\rho_{\text{reh}} = \frac{\pi^2}{30} g_{\text{reh}} T_{\text{reh}}^4. \quad (6)$$

The inflation ends when the first Hubble hierarchy parameter  $\epsilon_H = (3/2)(1+w) = 3K/(K+V) = \epsilon_{\text{end}}$ , therefore the kinetic energy  $K_{\text{end}} = \epsilon_{\text{end}} V_{\text{end}}/(3 - \epsilon_{\text{end}})$ , thus the total energy density  $\rho_{\text{end}} = K_{\text{end}} + V_{\text{end}} = 3V_{\text{end}}/(3 - \epsilon_{\text{end}})$ . The second equation above comes from direct calculation of  $\rho_{\text{reh}} = \rho_{\text{end}} \exp\left(-3 \int_{a_{\text{end}}}^{a_{\text{reh}}} (1+w_{\text{reh}}) d \ln a\right) = \rho_{\text{end}} e^{-3N_{\text{reh}}(1+w_{\text{reh}})}$ . Combining above three equations gives rise to

$$T_{\text{reh}}^4 = \frac{90V_{\text{end}}}{\pi^2(3 - \epsilon_{\text{end}})g_{\text{reh}}} e^{-3N_{\text{reh}}(1+w_{\text{reh}})}. \quad (7)$$

Inserting (7) into (3) gives the final expression for the third factor of (1).

The last factor  $H_*$  is usually fixed by Planck normalization  $A_s = H_*^2/8\pi^2\epsilon_*$ , namely,  $H_* = \pi\sqrt{r_* A_s}/2$ . However it requires full knowledge on tensor-to-scalar ratio  $r_*$  and the consistency relation  $r_* = 16\epsilon_*$ , both of which have not been observed or confirmed yet. A more conservative way to compute  $H_*$  is to use slow-roll equation

$$3H_*^2 = V_*. \quad (8)$$

Combining (2), (3) and (8) together gives the final formula for the effective number of degrees of freedom at the end of reheating phase

$$g_{\text{reh}} = \left( \frac{T_\gamma}{k_*} \right)^{12} \left( \frac{43}{11} \right)^4 \left( \frac{3 - \epsilon_{\text{end}}}{810} \right)^3 \left( \frac{\pi^6 V_*^6}{V_{\text{end}}^3} \right) \times \exp\left(9N_{\text{reh}} \left( w_{\text{reh}} - \frac{1}{3} \right) - 12N_*\right), \quad (9)$$

Nextly, we apply (9) for general single-field slow-roll inflationary potential  $V(\phi, p)$  with only one parameter  $p$  (for multi-parameter inflationary potential, one has to fix some of its parameters). The inflation ended when slow-roll condition is broken,

$$\epsilon(\phi_{\text{end}}, p) = \epsilon_{\text{end}} \Rightarrow \phi_{\text{end}}(p). \quad (10)$$

Once we have the field value of  $\phi_{\text{end}}(p)$  at the endpoint of inflation, we have the potential energy density at that moment

$$V(\phi_{\text{end}}(p), p) \equiv V_{\text{end}}(p). \quad (11)$$

To compute  $H_*$  via slow-roll equation  $3H_*^2 = V_*$ , one requires the field value of  $\phi_*$  when the pivot scale crosses the horizon. This can only be done by inputting Planck observations on the scalar power spectrum amplitude via

$$A_s = \frac{1}{24\pi^2} \frac{V(\phi_*, p)}{\epsilon(\phi_*, p)} \Rightarrow \phi_*(p). \quad (12)$$

Once we know field value of  $\phi_*(p)$  we have every information to restore  $H_* = \sqrt{V_*/3}$  by

$$V(\phi_*(p), p) \equiv V_*(p). \quad (13)$$

There is one more quantity to complete the evaluations, which is the  $e$ -folding number during inflation

$$\int_{\phi_{\text{end}}(p)}^{\phi_*(p)} \frac{V(\phi, p)}{V'_\phi(\phi, p)} d\phi \equiv N_*(p). \quad (14)$$

Combining (11), (13) and (14) together we have

$$g_{\text{reh}}(p, N_{\text{reh}}, w_{\text{reh}}) = \left( \frac{T_\gamma}{k_*} \right)^{12} \left( \frac{43}{11} \right)^4 \left( \frac{3 - \epsilon_{\text{end}}}{810} \right)^3 \frac{\pi^6 V_*^6(p)}{V_{\text{end}}^3(p)} \times \exp\left(9N_{\text{reh}} \left( w_{\text{reh}} - \frac{1}{3} \right) - 12N_*(p)\right). \quad (15)$$

Finally, three comments on (15) are as follows:

1. It can be tested that the general formalism presented above is insensitive to the precise values of  $\epsilon_{\text{end}}$  and  $g_{\text{reh}}$  due to the logarithmic dependence. Therefore it suffices to take fiducial values  $\epsilon_{\text{end}} = 1$ ,  $g_{\text{reh}} = 106.75$  for Higgs inflation and  $g_{\text{reh}} = 10^3$  for other single-field slow-roll inflationary models.

2. The  $w_{\text{reh}} = 1/3$  case should be seen as the equivalent case  $N_{\text{reh}} = 0$  which presents an instantaneous reheating process. We will see in the next section that an instantaneous reheating process manifests itself as an asymptotic line in the  $N_{\text{reh}}-w_{\text{reh}}$  plane.
3. The degeneracy between inflationary phase and reheating phase sources the freedom of choices of  $N_*$  in the  $n_s-r$  plane. This can be seen from the fact that any shift  $\Delta N_*$  from  $N_*$  can be compensated by the shifts  $\Delta N_{\text{reh}}$  and  $\Delta w_{\text{reh}}$  from  $N_{\text{reh}}$  and  $w_{\text{reh}}$  provided that  $9N_{\text{reh}}\Delta w_{\text{reh}} + 9\Delta N_{\text{reh}}(w_{\text{reh}} + \Delta w_{\text{reh}} - \frac{1}{3}) = 12\Delta N_*$ .

### III. REHEATING PHASE DIAGRAM

We start with the usual  $n_s-r$  plane. By solving following equations

$$A_s = \frac{1}{24\pi^2} \frac{V(\phi_*, p)}{\epsilon(\phi_*, p)}, \quad (16)$$

$$N_* = \int_{\phi_{\text{end}}(p)}^{\phi_*} \frac{V(\phi, p)}{V'(\phi, p)} d\phi, \quad (17)$$

with input value of  $A_s$ , one can express field value  $\phi_*(N_*)$  and potential parameter  $p(N_*)$  in terms of  $e$ -folding number  $N_*$  during inflation. Hence the inflationary predictions  $n_s(\phi_*(N_*), p(N_*)) \equiv n_s(N_*)$  and  $r(\phi_*(N_*), p(N_*)) \equiv r(N_*)$  can be made with respect to  $N_*$  in the  $n_s-r$  plane. However the reheating phase variables  $N_{\text{reh}}$  and  $w_{\text{reh}}$  can not be specified in this case in the  $n_s-r$  plane.

To break the degeneracy between inflationary phase and reheating phase as mentioned in the previous section, we propose to solve following equations

$$A_s = \frac{1}{24\pi^2} \frac{V(\phi_*, p)}{\epsilon(\phi_*, p)}, \quad (18)$$

$$g_{\text{reh}} = g_{\text{reh}}(p, N_{\text{reh}}, w_{\text{reh}}), \quad (19)$$

with input values of  $A_s$  and  $g_{\text{reh}}$ , and the obtained solutions  $\phi_*(N_{\text{reh}}, w_{\text{reh}})$  and  $p(N_{\text{reh}}, w_{\text{reh}})$  can be used to express inflationary observables like  $n_s(\phi_*(N_{\text{reh}}, w_{\text{reh}}), p(N_{\text{reh}}, w_{\text{reh}})) \equiv n_s(N_{\text{reh}}, w_{\text{reh}})$ ,  $r(\phi_*(N_{\text{reh}}, w_{\text{reh}}), p(N_{\text{reh}}, w_{\text{reh}})) \equiv r(N_{\text{reh}}, w_{\text{reh}})$  in terms of reheating phase variables  $N_{\text{reh}}$  and  $w_{\text{reh}}$ . Other quantities like  $N_*(p(N_{\text{reh}}, w_{\text{reh}})) \equiv N_*(N_{\text{reh}}, w_{\text{reh}})$  in (14), and  $T_{\text{reh}}(p(N_{\text{reh}}, w_{\text{reh}}), N_{\text{reh}}, w_{\text{reh}}) \equiv T_{\text{reh}}(N_{\text{reh}}, w_{\text{reh}})$  in (7) can also be expressed in terms of reheating phase variables  $N_{\text{reh}}$  and  $w_{\text{reh}}$ . Expressing various observables in terms of reheating phase variables  $N_{\text{reh}}$  and  $w_{\text{reh}}$  in the  $N_{\text{reh}}-w_{\text{reh}}$  plane will be referred as the *reheating phase diagrams*. It can be tested that the reheating phase diagrams are insensitive to different input values of  $g_{\text{reh}}$ .

What priors should we choose for  $N_{\text{reh}}$  and  $w_{\text{reh}}$  in general? Firstly, in the  $n_s-r$  plane the inflationary predictions are usually made by choosing  $N_{\text{inf}}$  in the range

[50, 60], which is actually degenerated with  $N_{\text{reh}}$ . Secondly, the inflation era ends when the EoS parameter equals to  $-1/3$  and the radiation era begins when the EoS parameter equals to  $1/3$ . It seems that  $w_{\text{reh}}$  should be in the range  $[-1/3, 1/3]$ . However it is possible to achieve potential dominance (with its EoS parameter equals to  $-1$ ) and kinetic dominance (with its EoS parameter equals to  $1$ ) assuming a massive inflaton. Therefore without preknowledge on the reheating phase, one can in general choose  $N_{\text{reh}}$  in the prior  $[0, 30]$  and  $w_{\text{reh}}$  in the prior  $[-1, 1]$ . A constant EoS parameter  $w_{\text{reh}}$  in this sense should be viewed as an effective parameter time-averaging the EoS parameter during the whole reheating process.

#### A. Reheating Phase Diagram for Higgs Inflation

In the Higgs inflation, the Higgs field with a large non-minimal coupling to Einstein gravity in Jordan frame can give rise to an exponential plateau-like potential in large field region in Einstein frame where the inflaton is defined. The action in Jordan frame is

$$S_J = \int d^4x \sqrt{-g} \left( \frac{M_{\text{P}}^2}{2} \Omega^2 R - \frac{1}{2} (\partial h)^2 - V(h) \right). \quad (20)$$

where  $V(h) = (\lambda/4)(h^2 - v^2)^2$  with VEV of EW vacuum  $v = 246\text{GeV}$ . Here the conformal factor

$$\Omega^2 = \frac{\tilde{g}_{\mu\nu}}{g_{\mu\nu}} = 1 + \frac{\xi h^2}{M_{\text{P}}^2}, \quad (21)$$

and the scalar field redefinition

$$\left( \frac{d\chi}{dh} \right)^2 = \frac{1}{\Omega^2} + \frac{6M_{\text{P}}^2}{\Omega^2} \left( \frac{d\Omega}{dh} \right)^2 \quad (22)$$

allow us to switch the action into Einstein frame

$$S_E = \int d^4x \sqrt{-\tilde{g}} \left( \frac{M_{\text{P}}^2}{2} \tilde{R} - \frac{1}{2} (\tilde{\partial}\chi)^2 - U(\chi) \right), \quad (23)$$

where the kinetic terms for Einstein gravity and the new scalar field are both canonically normalized. The potential term

$$U(\chi(h)) = \frac{V(h)}{\Omega^4} = \frac{\lambda M_{\text{P}}^4}{4\xi^2} \frac{\left( \frac{\xi h^2}{M_{\text{P}}^2} - \frac{\xi v^2}{M_{\text{P}}^2} \right)^2}{\left( 1 + \frac{\xi h^2}{M_{\text{P}}^2} \right)^2} \quad (24)$$

can be abbreviated as

$$U(\chi(\phi)) = \frac{Z}{4} \frac{\phi^4}{(1 + \phi^2)^2} \equiv V(\phi). \quad (25)$$

by using the dimensionless scalar field  $\phi = \sqrt{\xi}h/M_{\text{P}}$  and the combined parameter  $Z = \lambda/\xi^2$  for latter convenience. Here we ignore  $v$  and set  $M_{\text{P}}^2 = 1$  from now on. In the large field region  $h \gg M_{\text{P}}/\sqrt{\xi}$ , one

can solve the scalar field re-definition (22) to obtain  $\chi \simeq \sqrt{6}M_P \ln \sqrt{\xi}h/M_P \equiv \sqrt{6}M_P \ln \phi$ , thus an exponential plateau-like potential in large field region

$$U(\chi) = \frac{Z}{4} \left(1 + e^{-\frac{2\chi}{\sqrt{6}}}\right)^{-2} \quad (26)$$

is obtained as promised. The slow-roll dynamics with respect to the inflaton  $\chi$  can be carried out directly by computing the slow-roll parameters

$$\epsilon(\phi) = \frac{4}{3} \frac{1}{(\phi^2 + 1)^2}, \quad (27)$$

$$\eta(\phi) = -\frac{4}{3} \frac{1}{\phi^2 + 1} + \frac{4}{(\phi^2 + 1)^2}, \quad (28)$$

$$\zeta^2(\phi) = \frac{16/9}{(\phi^2 + 1)^2} - \frac{16}{(\phi^2 + 1)^3} + \frac{64/3}{(\phi^2 + 1)^4}, \quad (29)$$

the  $e$ -folding number during inflation

$$N(\phi_N) = \frac{3}{4} \left( \phi_N^2 - \phi_{\text{end}}^2 - \ln \frac{1 + \phi_N^2}{1 + \phi_{\text{end}}^2} \right), \quad (30)$$

the scalar spectral indexes and its running and the tensor-to-scalar ratio

$$n_s(\phi_N) = 1 - \frac{8}{3} \frac{1}{\phi_N^2 + 1}, \quad (31)$$

$$r(\phi_N) = \frac{64}{3} \frac{1}{(\phi_N^2 + 1)^2}, \quad (32)$$

$$\alpha_s(\phi_N) = -\frac{32}{9} \frac{1}{(\phi_N^2 + 1)^2} + \frac{32}{9} \frac{1}{(\phi_N^2 + 1)^3}. \quad (33)$$

in terms of dimensionless  $\phi$ .

The reheating phase diagrams with respect to  $n_s, r, \alpha_s, Z, T_{\text{reh}}, N_{\text{inf}}$  for Higgs inflation can be shown simultaneously in the Figure 1 with input values of  $g_{\text{reh}} = 106.75$  and  $\ln(10^{10}A_s) = 3.094 \pm 0.034$  from Planck 2015 normalization [2]. The dashed contour lines in the last panel are due to different input values of  $\ln(10^{10}A_s) = 3.094 \pm 0.034$  from Planck 2015 normalization [2]. However the dashed contour lines in other panels can not tell any difference from the solid contour lines. Therefore it suffices to take  $\ln(10^{10}A_s) = 3.094$  when other inflationary models are concerned. It can be seen in the first panel of Figure 1 that almost all possible reheating processes are allowed within the  $1\sigma$  region of  $n_s = 0.9645 \pm 0.0049$  reported by Planck 2015 TT,TE,EE+lowP [2]. This insensitivity of cosmological predictions on the reheating phase can also be shown in other panels too. Therefore the cosmological predictions (including reheating temperature as already shown in Ref. [18] in the  $n_s-r$  plane) of Higgs inflation are insensitive to its reheating processes given current precision of CMB measurements. However the reheating processes should be appreciated for the future measurement of  $n_s$  with refined precision up to 1% and direct detection of primordial gravitational wave.

## B. Reheating Phase Diagram for Other Models

The reheating phase diagram can be also applied to other single-field slow-roll inflationary models. Among those inflationary models selected by Planck collaboration [2], we choose to study power-law potential, hilltop inflation, natural inflation, SB SUSY inflation, and superconformal  $\alpha$  attractors E/T-models. Since the models closest to Higgs inflation (equivalent to  $R^2$  inflation to lowest order in slow-roll approximation at tree level) in terms of Bayes evidence are brane inflation and exponential inflation, we expect the outcome of these two models would be essentially the same as Higgs inflation. From now on, we adopt  $g_{\text{reh}} = 10^3$  and  $\ln(10^{10}A_s) = 3.094$ . It worth noting that in this subsection the reheating phase diagrams are only showed with respect to  $n_s$  and  $r$ , which are strongly constrained from Planck 2015.

### Power-law potential

Inflation models with power-law potential [19] motivated by axion monodromy [20, 21] take values, such as  $p = 4/3, 1, 2/3$  for

$$V(\phi) = \Lambda^4 \phi^p. \quad (34)$$

The slow-roll approximations give

$$\epsilon(\phi) = p^2/(2\phi^2), \quad (35)$$

$$\eta(\phi) = p(p-1)/\phi^2, \quad (36)$$

$$\phi_{\text{end}} = p/\sqrt{2}, \quad (37)$$

$$N = (\phi_N^2 - \phi_{\text{end}}^2)/(2p), \quad (38)$$

which are necessary to carry out their reheating phase diagrams in Figure 2. By requiring  $0.9547 < n_s < 0.9743$  and  $r < 0.1$  according to current constraints on inflation from Planck 2015 TT,TE,EE+lowP [2], one find the parameter spaces of its reheating phase specified by green color in the  $N_{\text{reh}}-w_{\text{reh}}$  plane. An interesting observation is that, inflation models with larger area of green region have larger Bayes factors shown in the Table 6 in the Ref.[2]. It is worth noting that the axion monodromy inflation with  $\phi^{2/3}$  potential, which lie at the edge of 95% confidence region in the  $n_s-r$  plane constrained by Planck 2015 TT,TE,EE+lowP, can actually meet the current constraints on inflation from Planck 2015 if the reheating processes [22] are taken into account. We did not present here the reheating phase diagrams for power-law potential with  $p \geq 2$  because their reheating phase diagrams simply have no green region at all (put it in other words, the regions allowed for  $0.9547 < n_s < 0.9743$  and regions allowed for  $r < 0.1$  have no intersection.).

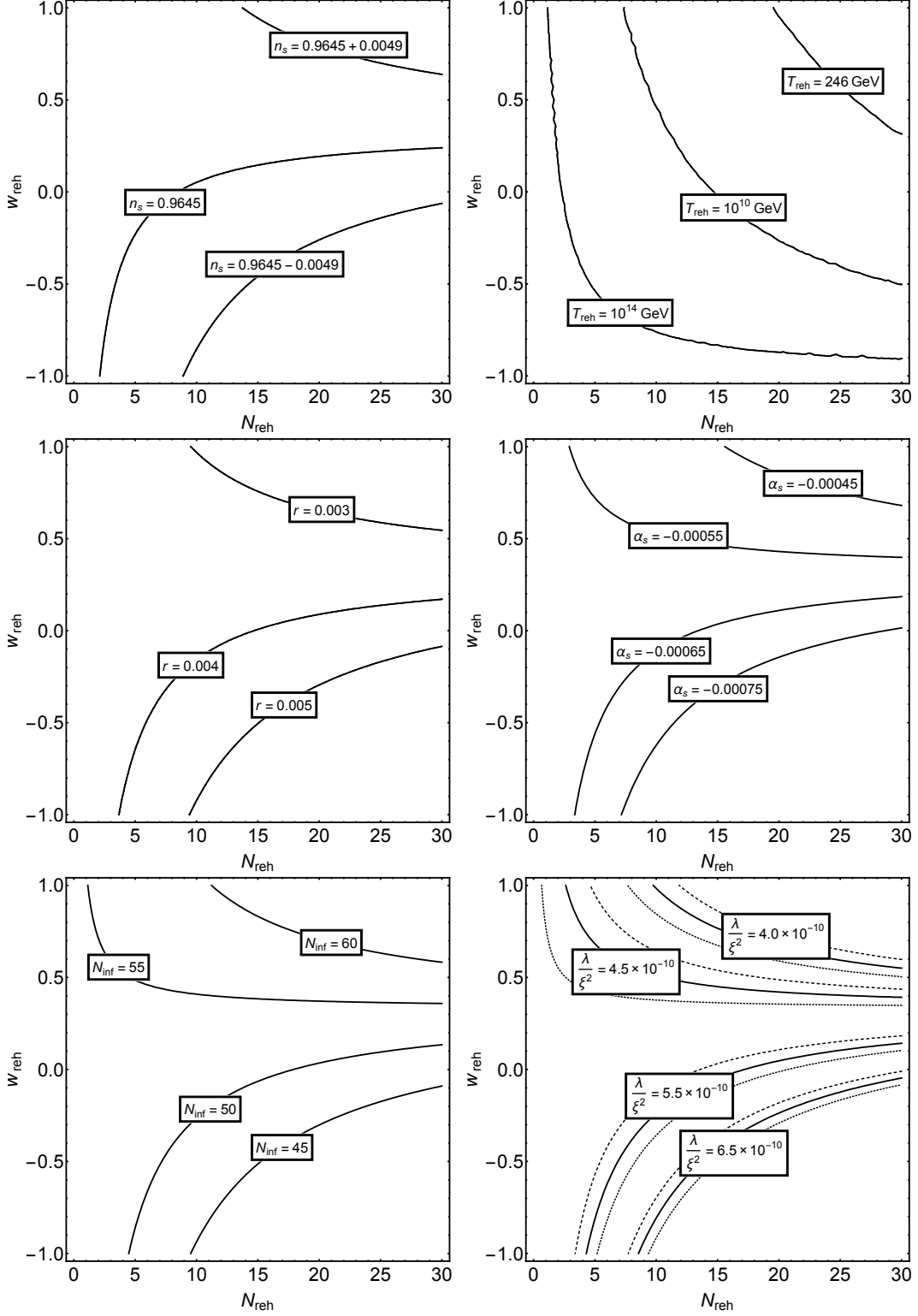


FIG. 1. Reheating phase diagrams for Higgs inflation. Cosmological predictions of  $n_s, r, \alpha_s, Z, T_{\text{reh}}, N_{\text{inf}}$  are drawn with respect to phase variables  $N_{\text{reh}}$  and  $w_{\text{reh}}$ . The dashed contour lines in the last panel are due to different input value of  $\ln(10^{10} A_s) = 3.094 \pm 0.034$  from Planck 2015 normalization [2]. It can be shown in the first panel that almost all possible reheating processes are allowed within the  $1\sigma$  region of  $n_s = 0.9645 \pm 0.0049$  reported by Planck 2015 TT,TE,EE+lowP [2]. This insensitivity of cosmological predictions on the reheating phase can also be shown in other panels too.

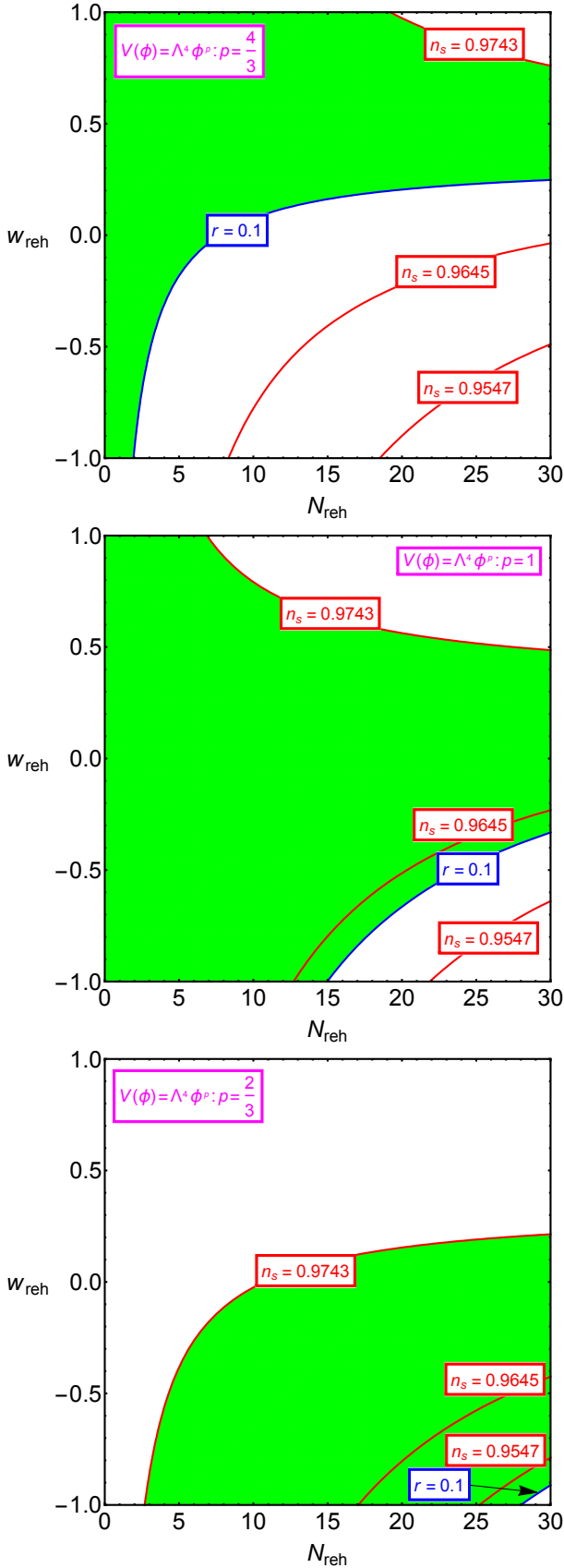


FIG. 2. Reheating phase diagrams for power-law potential with  $p = 4/3, 1, 2/3$  from the top down. The green colored region is specified by requiring  $0.9547 < n_s < 0.9743$  and  $r < 0.1$ .

### Hilltop inflation

Hilltop inflation [23] with inflationary potential

$$V(\phi) = \Lambda^4 \left( 1 - \frac{\phi^p}{\mu^p} + \dots \right) \quad (39)$$

considered here takes small field limit  $\phi \ll \mu$  with super-Planckian *vev*  $\mu \gg 1$ . The slow-roll approximations give

$$\epsilon_1(\phi) = -\frac{\dot{H}}{H^2} = \frac{p^2}{2\mu^2} \frac{(\phi/\mu)^{2p-2}}{(1 - (\phi/\mu)^p)^2}, \quad (40)$$

$$\epsilon_2(\phi) = \frac{\dot{\epsilon}_1}{H\epsilon_1} = \frac{2p}{\mu^2} \frac{p-1 + (\phi/\mu)^p}{(1 - (\phi/\mu)^p)^2} (\phi/\mu)^{p-2}, \quad (41)$$

$$\phi_{\text{end}} = \mu - 1/\sqrt{2} + (p-1)/(4\mu) + \mathcal{O}(1/\mu^2), \quad (42)$$

in addition with

$$N = \frac{\mu^2}{2p} \left[ \left( \frac{\phi_N}{\mu} \right)^2 - \left( \frac{\phi_{\text{end}}}{\mu} \right)^2 + \frac{2}{p-2} \left( \left( \frac{\phi_N}{\mu} \right)^{2-p} - \left( \frac{\phi_{\text{end}}}{\mu} \right)^{2-p} \right) \right], \quad (43)$$

for  $p \neq 2$  and

$$N = \frac{\mu^2}{4} \left[ \left( \frac{\phi_N}{\mu} \right)^2 - \left( \frac{\phi_{\text{end}}}{\mu} \right)^2 - 2 \ln \left( \frac{\phi_N/\mu}{\phi_{\text{end}}/\mu} \right) \right], \quad (44)$$

for  $p = 2$ . It was constrained at 95% CL that Planck 2015 favours hilltop inflation with  $\log_{10} \mu > 1.02(1.05)$  for  $p = 2, w_{\text{reh}} = 0$  (allowing  $w_{\text{reh}}$  to vary) and  $\log_{10} \mu > 1.05(1.02)$  for  $p = 4, w_{\text{reh}} = 0$  (allowing  $w_{\text{reh}}$  to vary). However, the reheating phase diagrams for hilltop inflation presented in Figure 3 slightly loose the bound on  $\log_{10} \mu$ . Each colored region is specified by requiring  $0.9547 < n_s < 0.9743$  and  $r < 0.1$  with respect to different values of parameter  $\mu$ . Larger values of  $\mu$  will cover larger part of parameter space in  $N_{\text{reh}}-w_{\text{reh}}$  plane. However lower value of  $\mu$  would require more exotic reheating processes beyond theoretically reasonable reheating processes with  $N_{\text{reh}} \sim \mathcal{O}(1)$  and  $w_{\text{reh}} \in [-1/3, 1/3]$ .

### Natural inflation

Natural inflation [24, 25] with periodic potential

$$V(\phi) = \Lambda^4 \left[ 1 + \cos \left( \frac{\phi}{f} \right) \right]. \quad (45)$$

As far as only  $n_s, r$  are concerned, natural inflation seems to recover the quadratic chaotic inflation when the scale of curvature of the potential  $f \rightarrow \infty$ . The slow-roll ap-

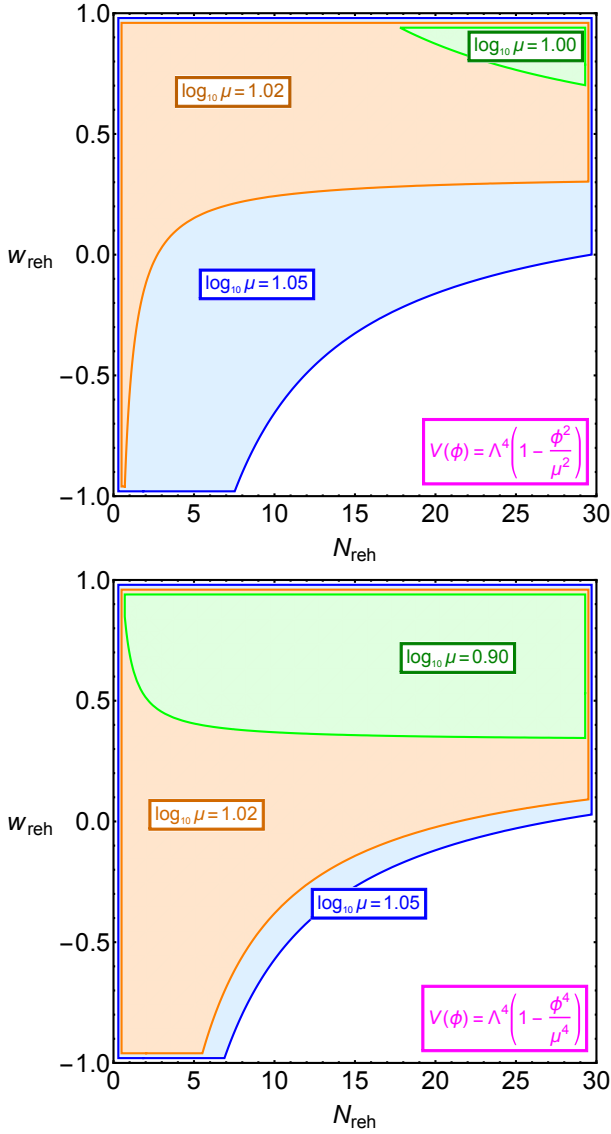


FIG. 3. Reheating phase diagrams for hilltop inflation with  $p = 2$  (upper panel) and  $p = 4$  (lower panel). Each colored region is specified by requiring  $0.9547 < n_s < 0.9743$  and  $r < 0.1$  with respect to different values of parameter  $\mu$ .

proximations give

$$\epsilon_1(\phi) = -\frac{\dot{H}}{H^2} = \frac{1}{2f^2} \frac{\sin^2(\phi/f)}{(1 + \cos(\phi/f))^2}, \quad (46)$$

$$\epsilon_2(\phi) = \frac{\dot{\epsilon}_1}{H\epsilon_1} = \frac{2}{f^2} \frac{1}{1 + \cos(\phi/f)}, \quad (47)$$

$$\phi_{\text{end}} = \arccos\left(\frac{1 - 2f^2}{1 + 2f^2}\right), \quad (48)$$

$$N = f^2 \ln\left(\frac{1 - \cos(\phi_{\text{end}}/f)}{1 - \cos(\phi_N/f)}\right), \quad (49)$$

which are necessary to carry out their reheating phase diagram in Figure 4. It was constrained at 95% CL that Planck 2015 favours natural inflation with  $\log_{10} f >$

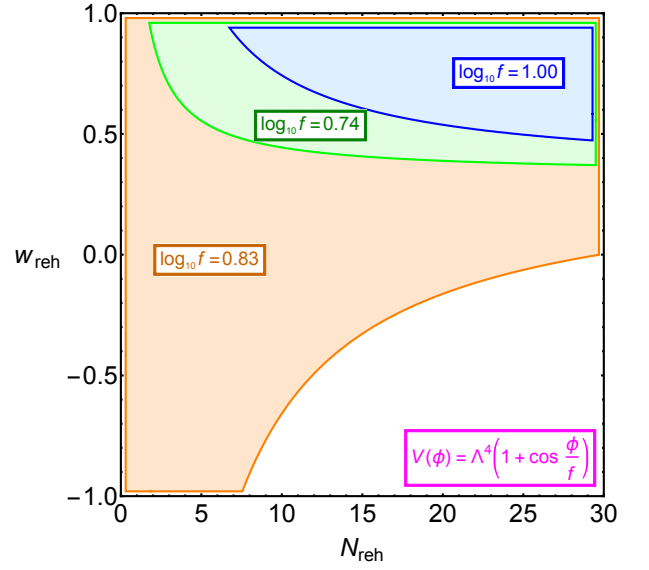


FIG. 4. Reheating phase diagrams for natural inflation. Each colored region is specified by requiring  $0.9547 < n_s < 0.9743$  and  $r < 0.1$  with respect to different values of parameter  $f$ .

0.84(0.83) for  $w_{\text{reh}} = 0$  (allowing  $w_{\text{reh}}$  to vary). As in the case of hilltop inflation, the reheating phase diagram presented in Figure 4 slightly loose the bound on  $\log_{10} f$ , and lower value of  $f$  will require more exotic reheating processes. However since there are temporarily no observational constraints on reheating phase variables, one can not simply rule out these parameter space.

#### Spontaneously broken SUSY

Spontaneously broken SUSY inflation [26] is described by the potential

$$V(\phi) = \Lambda^4(1 + \alpha_h \log \phi) \quad (50)$$

with a flat prior  $[-2.5, 1]$  for  $\log_{10} \alpha_h$ . The slow-roll approximations give

$$\epsilon(\phi) = \frac{\alpha_h^2}{2\phi^2(1 + \alpha_h \log \phi)^2}, \quad (51)$$

$$\eta(\phi) = -\frac{\alpha_h}{\phi^2(1 + \alpha_h \log \phi)}, \quad (52)$$

$$\phi_{\text{end}} = \sqrt{2}/\sqrt{W(2 \exp[2/\alpha_h])}, \quad (53)$$

$$N = \left(\frac{1}{2\alpha_h} - \frac{1}{4}\right)(\phi_N^2 - \phi_{\text{end}}^2) + \frac{1}{4}(\phi_N^2 \log \phi_N^2 - \phi_{\text{end}}^2 \log \phi_{\text{end}}^2). \quad (54)$$

Here  $W(z)$  is Lambert function by definition  $z = W(z) \exp[W(z)]$ . The reheating phase diagram for SB SUSY inflation is presented in Figure 5. As in the case of natural inflation, smaller values of  $\alpha_h$  are allowed if one invokes more exotic reheating processes. Although

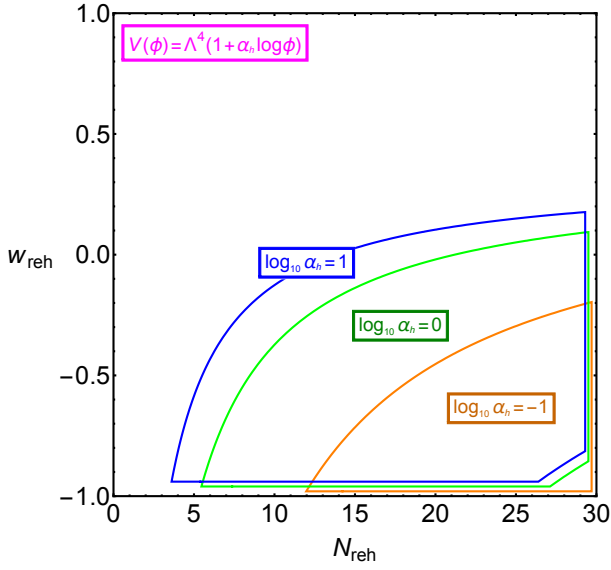


FIG. 5. Reheating phase diagrams for SB SUSY inflation. Each colored region is specified by requiring  $0.9547 < n_s < 0.9743$  and  $r < 0.1$  with respect to different values of parameter  $\alpha_h$ .

SB SUSY inflation lies outside 95% confidence region in  $n_s$ - $r$  plane constrained by Planck 2015 TT,TE,EE+lowP, there exist parameter spaces of reheating phase in  $N_{\text{reh}}$ - $w_{\text{reh}}$  plane to accommodate the Planck's constraints on inflation. Therefore SB SUSY inflation can not be simply ruled out if the reheating phase is taken into account.

#### $\alpha$ attractors

$\alpha$  attractors E-models [27] with exponentially flat potential

$$V(\phi) = \Lambda^4 \left( 1 - e^{-\frac{2\phi}{\sqrt{6}\alpha}} \right)^2 \quad (55)$$

approaches the predictions on  $(n_s, r)$  of quadratic inflation for  $\alpha \rightarrow \infty$  and Starobinsky model ( $n_s = 1 - 2/N, r = 12/N^2$ ) for  $\alpha = 1$  and  $\alpha$ -attractors ( $n_s = 1 - 2/N, r = 0$ ) for  $\alpha \rightarrow 0$ . Planck 2015 favours  $\alpha$  attractors E-models with  $\log_{10} \alpha^2 < 1.7(2.0)$  for  $w_{\text{reh}} = 0$  (allowing  $w_{\text{reh}}$  to vary). However the reheating phase diagram presented in Figure 6 slightly loosens the bound on  $\alpha$  as expected.

$\alpha$  attractors T-models [27] with inflationary potential

$$V(\phi) = \Lambda^4 \tanh^{2m} \left( \frac{\phi}{\sqrt{6}\alpha} \right) \quad (56)$$

approaches the predictions on  $(n_s, r)$  of power-law potential  $\phi^{2m}$  for  $\alpha \rightarrow \infty$  and  $\alpha$ -attractors ( $n_s = 1 - 2/N, r = 0$ ) for  $\alpha \rightarrow 0$ . Planck 2015 favours  $\alpha$  attractors T-models with  $\log_{10} \alpha^2 < 2.3(2.5)$  for  $m = 1, w_{\text{reh}} = 0$  (allowing  $w_{\text{reh}}$  to vary) and  $0.2 < m < 1 (m < 1)$  for

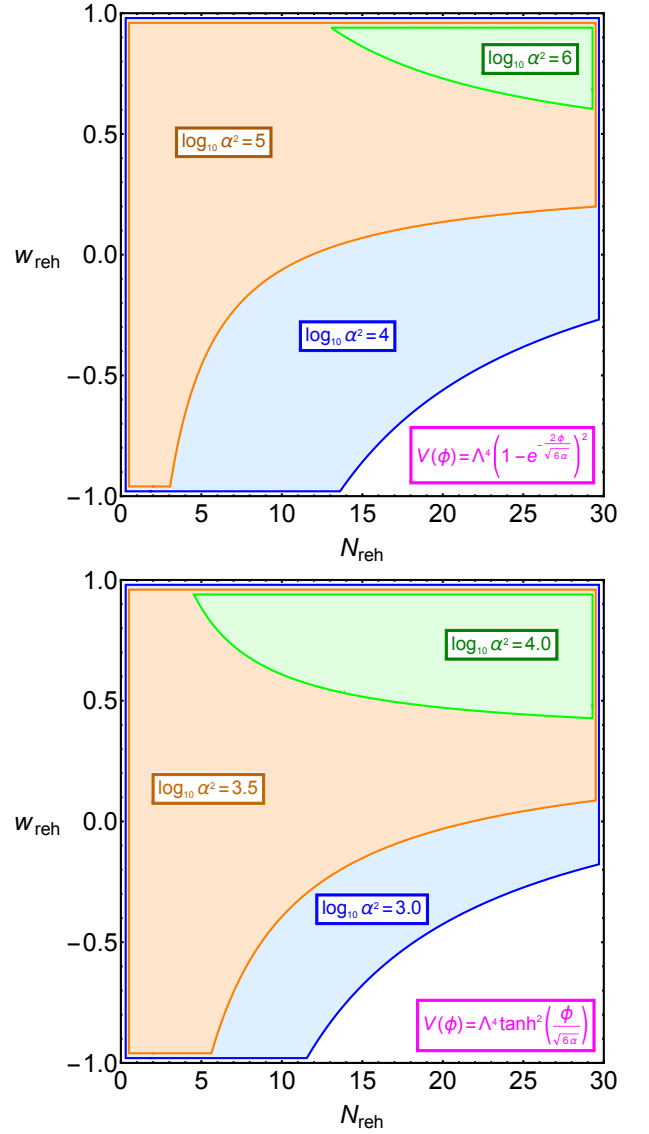


FIG. 6. Reheating phase diagrams for  $\alpha$  attractors E-model (upper panel) and T-model (lower panel) with  $m = 1$ . Each colored region is specified by requiring  $0.9547 < n_s < 0.9743$  and  $r < 0.1$  with respect to different values of parameter  $\alpha$ .

$m \neq 1, w_{\text{reh}} = 0$  (allowing  $w_{\text{reh}}$  to vary). However the reheating phase diagram presented in Figure 6 slightly loosens the bound on  $\alpha$  as expected.

## IV. CONCLUSIONS

In  $n_s$ - $r$  plane one usually characterizes the uncertainties from reheating phase by the choice of freedom on the  $e$ -folding number of inflation. In this paper we characterize the reheating phase by only two effective parameters  $N_{\text{reh}}$  and  $w_{\text{reh}}$ . Thanks to the fact that observable quantities are insensitive to the effective number of degrees of freedom at the end of reheating phase, we are able



to express all other inflationary observables in terms of the phase variables  $N_{\text{reh}}$  and  $w_{\text{reh}}$ . Therefore for the first time we are able to constrain the parameter space of reheating phase in the  $N_{\text{reh}}-w_{\text{reh}}$  plane with respect to the constraints on inflation from Planck 2015. For Higgs inflation, the parameter space of reheating phase covers almost all the  $N_{\text{reh}}-w_{\text{reh}}$  plane, indicating that inflationary predictions of Higgs inflation are insensitive to its reheating process given current precision of CMB measurements. However future refined measurements on scalar spectral index and direct detection of primordial gravitational wave will constrain the reheating phase variables. For other inflationary models selected by Planck collaboration, the constrained parameter spaces of reheating phase generally loose the bound on the potential parameters if more exotic reheating processs are allowed. Inflationary models with larger parameter spaces in the reheating phase diagrams generally appear with larger Bayes factors. Since there are only theoretical considerations, not the observational constraints on the possible reheating phase, one can not simply rule out those parameter space of reheating phase with exotic reheating processs even if they lie outside 95% confidence region in  $n_s-r$  plane constrained by Planck 2015 TT,TE,EE+lowP. Only those inflationary models with no allowed param-

eter space of reheating phase in the  $N_{\text{reh}}-w_{\text{reh}}$  plane can be certainly ruled out.

*Note added* The paper [18] showed up on arXiv while we were preparing our first version of manuscript. We both follow the same method to study similar problem for Higgs inflation but with different angle. We characterize the reheating phase with  $N_{\text{reh}}$  and  $w_{\text{reh}}$  and express every other observables in terms of these two phase variables. The impact from various reheating processs on the inflationary predictions not only can be shown with respect to the reheating temperature but also other cosmological observables. We further study other inflationary models selected by Planck Collaboration, and find that the reheating phase diagram can be used to constrain the parameter space of reheating phase to meet current constraints on inflation.

## ACKNOWLEDGMENTS

We would like to thank Peng-Xu Jiang and Jian-Wei Hu for helpful discussions. RGC is supported by the Strategic Priority Research Program of the Chinese Academy of Sciences, Grant No.XDB09000000. ZKG is supported by the National Natural Science Foundation of China No.11175225 and No.11335012.

- 
- [1] P. Ade *et al.* (Planck Collaboration), *Astron.Astrophys.* **571**, A22 (2014), arXiv:1303.5082 [astro-ph.CO].
  - [2] P. Ade *et al.* (Planck Collaboration), (2015), arXiv:1502.02114 [astro-ph.CO].
  - [3] D. I. Podolsky, G. N. Felder, L. Kofman, and M. Peloso, *Phys.Rev.* **D73**, 023501 (2006), arXiv:hep-ph/0507096 [hep-ph].
  - [4] J. Martin and C. Ringeval, *Phys.Rev.* **D82**, 023511 (2010), arXiv:1004.5525 [astro-ph.CO].
  - [5] J. Martin, C. Ringeval, and R. Trotta, *Phys.Rev.* **D83**, 063524 (2011), arXiv:1009.4157 [astro-ph.CO].
  - [6] J. Martin, C. Ringeval, and V. Vennin, *Phys.Dark Univ.* (2014), 10.1016/j.dark.2014.01.003, arXiv:1303.3787 [astro-ph.CO].
  - [7] J. Martin, C. Ringeval, R. Trotta, and V. Vennin, *JCAP* **1403**, 039 (2014), arXiv:1312.3529 [astro-ph.CO].
  - [8] J. Martin, C. Ringeval, and V. Vennin, *JCAP* **1410**, 038 (2014), arXiv:1407.4034 [astro-ph.CO].
  - [9] J. Martin, C. Ringeval, and V. Vennin, *Phys.Rev.Lett.* **114**, 081303 (2015), arXiv:1410.7958 [astro-ph.CO].
  - [10] L. Dai, M. Kamionkowski, and J. Wang, *Phys.Rev.Lett.* **113**, 041302 (2014), arXiv:1404.6704 [astro-ph.CO].
  - [11] P. Creminelli, D. L. Nacir, M. Simonović, G. Trevisan, and M. Zaldarriaga, *Phys.Rev.* **D90**, 083513 (2014), arXiv:1405.6264 [astro-ph.CO].
  - [12] J. B. Munoz and M. Kamionkowski, *Phys.Rev.* **D91**, 043521 (2015), arXiv:1412.0656 [astro-ph.CO].
  - [13] J. L. Cook, E. Dimastrogiovanni, D. A. Easson, and L. M. Krauss, *JCAP* **1504**, 047 (2015), arXiv:1502.04673 [astro-ph.CO].
  - [14] F. L. Bezrukov and M. Shaposhnikov, *Phys.Lett.* **B659**, 703 (2008), arXiv:0710.3755 [hep-th].
  - [15] F. Bezrukov, D. Gorbunov, and M. Shaposhnikov, *JCAP* **0906**, 029 (2009), arXiv:0812.3622 [hep-ph].
  - [16] J. Garcia-Bellido, D. G. Figueroa, and J. Rubio, *Phys.Rev.* **D79**, 063531 (2009), arXiv:0812.4624 [hep-ph].
  - [17] F. Bezrukov, J. Rubio, and M. Shaposhnikov, (2014), arXiv:1412.3811 [hep-ph].
  - [18] J.-O. Gong, S. Pi, and G. Leung, (2015), arXiv:1501.03604 [hep-ph].
  - [19] A. D. Linde, *Phys.Lett.* **B129**, 177 (1983).
  - [20] E. Silverstein and A. Westphal, *Phys.Rev.* **D78**, 106003 (2008), arXiv:0803.3085 [hep-th].
  - [21] L. McAllister, E. Silverstein, and A. Westphal, *Phys.Rev.* **D82**, 046003 (2010), arXiv:0808.0706 [hep-th].
  - [22] H. B. Moghaddam and R. Brandenberger, (2015), arXiv:1502.06135 [hep-th].
  - [23] L. Boussekeur and D. Lyth, *JCAP* **0507**, 010 (2005), arXiv:hep-ph/0502047 [hep-ph].
  - [24] K. Freese, J. A. Frieman, and A. V. Olinto, *Phys.Rev.Lett.* **65**, 3233 (1990).
  - [25] F. C. Adams, J. R. Bond, K. Freese, J. A. Frieman, and A. V. Olinto, *Phys.Rev.* **D47**, 426 (1993), arXiv:hep-ph/9207245 [hep-ph].
  - [26] G. Dvali, Q. Shafi, and R. K. Schaefer, *Phys.Rev.Lett.* **73**, 1886 (1994), arXiv:hep-ph/9406319 [hep-ph].
  - [27] R. Kallosh, A. Linde, and D. Roest, *JHEP* **1311**, 198 (2013), arXiv:1311.0472 [hep-th].